Vision-Based Robotic Grasping and Manipulation of USB Wires

Conference Paper · May 2018

DOI: 10.1109/ICRA.2018.8460694

4 authors, including:

Xiang Li
Tsinghua University
61 PUBLICATIONS **719** CITATIONS
SEE PROFILE

Yuan Gao
The Chinese University of Hong Kong
4 PUBLICATIONS **6** CITATIONS
SEE PROFILE

Yun Liu
Chang Gung University
342 PUBLICATIONS **7,793** CITATIONS
SEE PROFILE

Vision-Based Robotic Grasping and Manipulation of USB Wires

Xiang Li, Xing Su, Yuan Gao, and Yun-Hui Liu

***Abstract*— The fast expanding 3C (Computer, Communication, and Consumer electronics) manufacturing leads to a high demand on the fabrication of USB cables. While several commercial machines have been developed to automate the process of stripping and soldering of USB cables, the operation of manipulating USB wires according to the color code is heavily dependent on manual works because of the deformation property of wires, probably resulting in the falling-off or the escape of wires during manipulation. In this paper, a new vision-based controller is proposed for robotic grasping and manipulation of USB wires. A novel two-level structure is developed and embedded into the controller, where *Level-I* is referred to as the grasping and manipulation of wires, and *Level-II* is referred to as the wire alignment by following the USB color code. The proposed formulation allows the robot to automatically grasp, manipulate, and align the wires in a sequential, simultaneous, and smooth manner, and hence to deal with the deformation of wires. The dynamic stability of the closed-loop system is rigorously proved with Lyapunov methods, and experiments are performed to validate the proposed controller.**

I. Introduction

The USB cable is a very common and important accessory for 3C products (Computer, Communication, and Consumer electronics), for purposes of charging and data transfer. The fast expanding 3C manufacturing leads to a high demand on the fabrication of USB cables. For example, the *iPhone* sales in the fourth quarter of 2016 are estimated as 76 $million$ [1], that is, 76 $million$ pieces of USB charger cables are sold in one quarter. Considering the USB cables for other mobiles and smart devices, the demand would be even larger.

A typical USB-cable soldering process consists of three steps. First, the cable sheath is stripped. Second, the four wires are fixed and aligned in a desired sequence. Third, the wires and the USB head are soldered together. Commercial machines have been developed to automate the first [2] and the third steps [3], but the second step is still heavily dependent on manual works, which has the disadvantages of low speed, low efficiency, and low output. Upgrading the current manual works with robotic technology can address the problems. However, most robotic manipulation techniques are limited to the manipulation of rigid objects [4], [5]. Due to the property of deformation, manipulating the USB wires is more challenging. In particular, the shape of wires is easily changed under applied forces, which may result in the falling-off during the manipulation.

Several robotic manipulation techniques have been reported in the literature to deal with the deformation of soft objects [6]–[12]. In [6], a control scheme was proposed to actively shape soft food dough by using a forming process model of rheological food dough. In [7], an active shaping method was developed for the 1-D deformation of rheological material. In [8], a controller was presented for the manipulation of soft objects with multiple robot arms, by specifying the control objective as a desired contour. The aforementioned results [6]–[8] commonly require model identification or calibration prior to the manipulation task. By exploring the property of *diminishing rigidity*, a model-free controller was proposed in [9] for manipulating a specific class of soft objects such as fabrics and ropes. By constructing regressors based on the structure of deformation model, a series of active deformation controllers were proposed in [10]–[12], such that the parameters of the deformation model of soft objects can be estimated online. In [13], [14], it was shown that PID control plus dynamic compensation for multiple robots can manipulate flexible beams to the desired position and the desired orientation. Most of existing results are limited at kinematic level [9]–[12], where the manipulation speed is low and not suitable for 3C manufacturing. In addition, it is implicitly assumed that the contact between the robot end effector and the soft object is always maintained, and hence the methods become invalid whenever the contact is lost.

This paper considers the problem of robotic grasping and manipulation of USB wires. In particular, a vision-based controller is proposed by organizing the control objective in a two-level structure. At *Level-I*, the robot grasps then manipulates a specific wire; At *Level-II*, the robot aligns the wires by referring to the USB color code. The two-level structure is embedded into the controller, and the transition among multiple operations (i.e. *Grasping*, *Manipulation*, *Alignment*) is smooth and simultaneous, which is realized by assessing the status of deformation. Such formulation guarantees the feasibility and the autonomous capability of robotic manipulation of USB wires. The dynamic stability of the closed-loop system is rigorously proved using Lyapunov methods. Experimental results in different scenarios are presented to validate the proposed controller. Note that the shape of USB wires is not necessarily to be controlled during manipulation, and hence the objective of the proposed controller is different from the active deformation [10]–[12].

II. Background

A. Problem Formulation

A USB cable comprises four wires with different colors (i.e. red, white, green, and black), which are enclosed by a sheath as illustrated in Fig. 1(a). Soldering the USB cable consists of several steps: i) stripping the sheath; ii)

The authors are with the Department of Mechanical and Automation Engineering, The Chinese University of Hong Kong, Hong Kong. This work was supported in part by the Innovation and Technology Commission of Hong Kong under Grant no. ITS/074/17 and in part by the Science and Technology Innovation Council of Shenzhen under Grant no. 20170480.

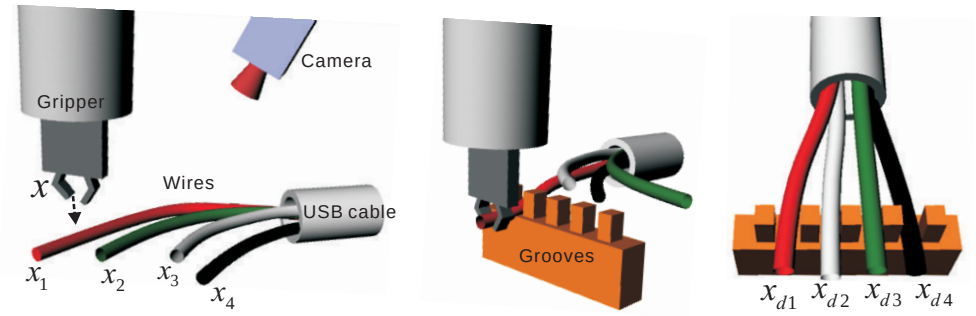

Fig. 1. Vision-based robotic manipulation of USB wires: (a) *Grasping*: The wire is to be grasped; (b) *Manipulation*: The wire is fixed at a designated groove; (c) *Alignment*: The wires are aligned according to the color code, i.e. $Red \rightarrow White \rightarrow Green \rightarrow Black$ (from left to right).

manipulating the wires; iii) soldering. In particular, step ii) is to fix and properly align the wires by following the color code (i.e. $Red \rightarrow White \rightarrow Green \rightarrow Black$). While several automatic machines have been developed for step i) and step iii), step ii) is still dependent on manual works.

This paper aims to upgrade the current manual works with robotic technology. Consider a vision-based robotic manipulation system illustrated in Fig. 1, where a camera is installed to measure the position of USB wires in image space, and a robot end effector (e.g. gripper) is controlled to manipulate the wires with visual feedback. In Fig. 1, $\boldsymbol{x}=[x_1, x_2]^T \in \Re^2$ is the position of the gripper in image space, $\boldsymbol{x}_i=[x_{i_1}, x_{i_2}]^T \in \Re^2$ denotes the position of the ith wire ($i = 1, 2, 3, 4$) corresponding to the colors of $Red, White, Green, Black$ respectively, $\boldsymbol{x}_{di} = [x_{di_1}, x_{di_2}]^T \in \Re^2$ is the desired position for the ith wire, which is also the corresponding groove.

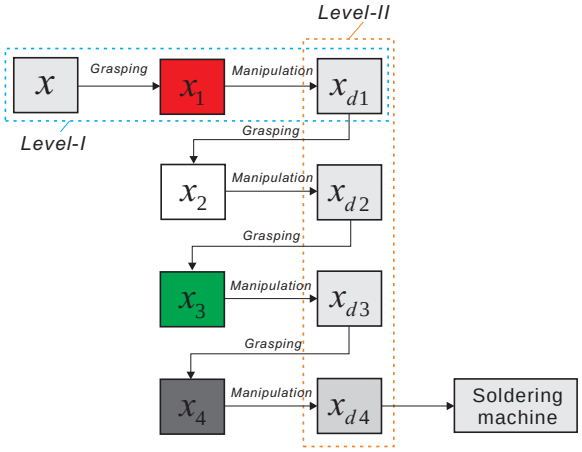

Fig. 2. A two-level structure of robotic manipulation of USB wires. *Level-I*: Grasping then manipulation; *Level-II*: Wire alignment by following $Red \rightarrow White \rightarrow Green \rightarrow Black$.

The robotic manipulation of USB wires is illustrated in Fig. 1, including i) *Grasping*: the gripper is controlled to grasp the wire; ii) *Manipulation*: the wire is manipulated and fixed at the designated groove; iii) *Alignment*: the four wires are aligned according to the color code. Then, the wires will be delivered to an automatic soldering machine. Due to the deformation of USB wires, the wire may fall off from the gripper during *Manipulation*, or it may escape from the grooves during *Alignment*.

To deal with the aforementioned problems, a two-level structure of sequential operations is formulated as illustrated in Fig. 2. At *Level-I*, a higher priority is assigned to *Grasping* such that the wire is always grasped before *Manipulation*, and *Grasping* is re-activated whenever the physical contact is lost; At *Level-II*, a highest priority is assigned to the Red color followed by $White, Green, Black$, to guarantee that the $i-1$ wires have been stably fixed at the desired positions before *Alignment* for the ith wire. The automatic and simultaneous transition between two levels ensures the feasibility of robotic manipulation of USB wires.

B. Robot Kinematics and Dynamics

The relationship between the task space of the gripper and the image space of the camera is defined by the pinhole camera model [15], [16]. Based on the pinhole camera model, the image-space velocity of the gripper can be related with the joint-space velocity as [5], [17]:

$$\dot{\boldsymbol{x}} = \boldsymbol{J}(\boldsymbol{q})\dot{\boldsymbol{q}}, \tag{1}$$

where $\boldsymbol{q} \in \Re^n$ is the vector of joint angles, n is the number of degrees of freedom, $\boldsymbol{J}(\boldsymbol{q}) \in \Re^{2\times n}$ is the image Jacobian matrix. In this paper, it is assumed that the camera is well calibrated such that $\boldsymbol{J}(\boldsymbol{q})$ is known.

Next, the dynamic model of the robot is given as [4], [18]:

$$\boldsymbol{M}(\boldsymbol{q})\ddot{\boldsymbol{q}}+\boldsymbol{C}(\dot{\boldsymbol{q}}, \boldsymbol{q})\dot{\boldsymbol{q}}+\boldsymbol{g}(\boldsymbol{q})=\boldsymbol{\tau}+\boldsymbol{\tau}_e, \tag{2}$$

where $\boldsymbol{M}(\boldsymbol{q}) \in \Re^{n\times n}$ represents the inertia, $\boldsymbol{C}(\dot{\boldsymbol{q}}, \boldsymbol{q})\dot{\boldsymbol{q}} \in \Re^n$ represents the centripetal and Coriolis torque, $\boldsymbol{g}(\boldsymbol{q}) \in \Re^n$ denotes the gravitational torque, $\boldsymbol{\tau} \in \Re^n$ denotes the control input, and $\boldsymbol{\tau}_e \in \Re^n$ represents the interaction torque between the gripper and the USB wires. Some important properties of the dynamic model (2) are listed as follows [4], [5], [18]:

i) The parameters $\boldsymbol{M}(\boldsymbol{q})$, $\boldsymbol{C}(\dot{\boldsymbol{q}}, \boldsymbol{q})$, $\boldsymbol{g}(\boldsymbol{q})$ are bounded;
ii) The matrix $\boldsymbol{M}(\boldsymbol{q})$ is positive definite;
iii) The matrix $\dot{\boldsymbol{M}}(\boldsymbol{q})-2\boldsymbol{C}(\dot{\boldsymbol{q}}, \boldsymbol{q})$ is skew-symmetric;

Note that the interaction torque is zero when the gripper does not grasp the wires and it is also bounded during *Grasping* and *Alignment*. It is also assumed that the dynamic parameters can be identified with sufficient accuracy.

III. Robotic Manipulation of USB Wires

In this section, a vision-based control method is developed for robotic grasping and manipulation of USB wires, where the control objective is formulated in the two-level structure. In particular, a novel composite vector is introduced, and the convergence to the composite vector ensures the realization of sequential operations at both levels.

A. Wire Grasping and Manipulation

Consider the sequential operation at *Level-I*, i.e. grasping then manipulation. First, a region function is formulated to specify the relative position between the robotic gripper and the ith wire as:

$$f_i(\boldsymbol{x}, \boldsymbol{x}_i) = ||\boldsymbol{x} - \boldsymbol{x}_i||^2 - \delta_I^2, \tag{3}$$

where δ_I is a very small positive constant. If the gripper is far away for the ith wire, $||\boldsymbol{x}-\boldsymbol{x}_i|| > \delta_I$, $f_i(\boldsymbol{x}, \boldsymbol{x}_i) > 0$. When the gripper stably grasps the wire such that $||\boldsymbol{x}-\boldsymbol{x}_i|| \leq \delta_I$, $f_i(\boldsymbol{x}, \boldsymbol{x}_i) \leq 0$.

Next, a weighting function for the ith wire is constructed to qualitatively describe the grasping status as:

$$w_i(\boldsymbol{x}, \boldsymbol{x}_i) = 1 - \frac{\{\min[0,[\min(0, f_i(\boldsymbol{x},\boldsymbol{x}_i))]^4 - ((\kappa_I \delta_I)^2 - \delta_I^2)^4]\}^4}{((\kappa_I \delta_I)^2 - \delta_I^2)^{16}}, \tag{4}$$

where $0 < \kappa_I < 1$ is a constant. From (4), $w_i(\boldsymbol{x}, \boldsymbol{x}_i) = 0$ where $f_i(\boldsymbol{x}, \boldsymbol{x}_i) > 0$, i.e. the ith wire is not grasped, and $w_i(\boldsymbol{x}, \boldsymbol{x}_i) = 1$ where $f_i(\boldsymbol{x}, \boldsymbol{x}_i) \leq 0$, that is, the grasping is guaranteed. Note that the order of the weighting function is set as 4 such that it is second-order continuous and hence the transition between 0 and 1 is smooth.

Using the weighting function, a composite vector is proposed for the ith wire as:

$$\boldsymbol{x}_{ci} = w_i(\boldsymbol{x}, \boldsymbol{x}_i)\boldsymbol{x}_{di} + (1 - w_i(\boldsymbol{x}, \boldsymbol{x}_i))\boldsymbol{x}_i. \tag{5}$$

Note that $\dot{\boldsymbol{x}}_{di} \equiv \boldsymbol{0}$. From (5), the composite vector is the current position of the ith wire when it is not grasped ($w_i(\boldsymbol{x}, \boldsymbol{x}_i) = 0$, $\boldsymbol{x}_{ci} = \boldsymbol{x}_i$), and it becomes the corresponding desired position when the wire is grasped by the gripper ($w_i(\boldsymbol{x}, \boldsymbol{x}_i) = 1$, $\boldsymbol{x}_{ci} = \boldsymbol{x}_{di}$). Differentiating $\boldsymbol{x}_{ci}$ with respect to time, we have: $\dot{\boldsymbol{x}}_{ci} = \dot{w}_i(\boldsymbol{x}, \boldsymbol{x}_i)\boldsymbol{x}_{di} - \dot{w}_i(\boldsymbol{x}, \boldsymbol{x}_i)\boldsymbol{x}_i + (1 - w_i(\boldsymbol{x}, \boldsymbol{x}_i))\dot{\boldsymbol{x}}_i$. Note that $\dot{w}_i(\boldsymbol{x}, \boldsymbol{x}_i) = 0$ when $w_i(\boldsymbol{x}, \boldsymbol{x}_i)$ is equal to 0 or 1. When $0 < w_i(\boldsymbol{x}, \boldsymbol{x}_i) < 1$, the wire has been grasped by the gripper, and thus $\dot{\boldsymbol{x}} \approx \dot{\boldsymbol{x}}_i$, $\dot{w}_i(\boldsymbol{x}, \boldsymbol{x}_i) = (\dot{\boldsymbol{x}} - \dot{\boldsymbol{x}}_i)^T [\frac{\partial w_i(\boldsymbol{x}, \boldsymbol{x}_i)}{\partial (\boldsymbol{x} - \boldsymbol{x}_i)}]^T$ is bounded since $\frac{\partial w_i(\boldsymbol{x}, \boldsymbol{x}_i)}{\partial (\boldsymbol{x} - \boldsymbol{x}_i)}$ is bounded. In addition, $\dot{\boldsymbol{x}}_i$ is also bounded where $0 < w_i(\boldsymbol{x}, \boldsymbol{x}_i) < 1$, since the wire is just grasped and at the beginning of the movement to the desired position with limited speed. Therefore, $\dot{\boldsymbol{x}}_{ci}$ is always bounded.

The composite vector (5) can be treated as a weighted summation between the position of the ith wire and the desired position, and the convergence of $\boldsymbol{x} \to \boldsymbol{x}_{ci}$ allows the robot to automatically grasp the wire then fix it at the groove, as $\boldsymbol{x}_{ci}$ transits between $\boldsymbol{x}_{ci} = \boldsymbol{x}_i$ (the objective of *Grasping*) and $\boldsymbol{x}_{ci} = \boldsymbol{x}_{di}$ (the objective of *Manipulation*) according to the relative position between the gripper and the wire. Note that the *Manipulation* is triggered after the wire is stably grasped, that is, higher priority is assigned to the *Grasping*. Whenever the contact between the gripper and the wire is lost during the manipulation, the *Grasping* is activated again to re-grasp the wire.

B. Wire Alignment

Consider the sequential operation at *Level-II*, i.e. wire alignment by following $Red \to White \to Green \to Black$. First, another series of region functions are formulated to specify the relative position between the grasped wire and the designated groove (the desired position) as:

$$h_i(\boldsymbol{x}_i, \boldsymbol{x}_{di}) = ||\boldsymbol{x}_i - \boldsymbol{x}_{di}||^2 - \delta_{II}^2, \tag{6}$$

where δ_{II} is also a very small constant. If the ith subwire is not located at its desired position, $||\boldsymbol{x}_i - \boldsymbol{x}_{di}|| > \delta_{II}$, $h_i(\boldsymbol{x}_i, \boldsymbol{x}_{di}) > 0$. When the wire stays at the designated groove, $||\boldsymbol{x}_i - \boldsymbol{x}_{di}|| \leq \delta_{II}$, $h_i(\boldsymbol{x}_i, \boldsymbol{x}_{di}) \leq 0$.

Then, another weighting function is given for as:

$$a_i(\boldsymbol{x}_i, \boldsymbol{x}_{di}) = \frac{\{\min[0,[\min(0, h_i(\boldsymbol{x}_i,\boldsymbol{x}_{di}))]^4 - ((\kappa_{II} \delta_{II})^2 - \delta_{II}^2)^4]\}^4}{((\kappa_{II} \delta_{II})^2 - \delta_{II}^2)^{16}}, \tag{7}$$

where $0 < \kappa_{II} < 1$ is a constant. From (7), $a_i(\boldsymbol{x}_i, \boldsymbol{x}_{di})$ is equal to 1 where $h_i(\boldsymbol{x}_i, \boldsymbol{x}_{di}) > 0$, and vice versa. The weighting function $a_i(\boldsymbol{x}_i, \boldsymbol{x}_{di})$ is also second-order continuous, and the transition between 0 and 1 is smooth.

Next, the overall composite vector is given as:

$$\begin{aligned}
\boldsymbol{x}_o = {} & a_1(\boldsymbol{x}_1, \boldsymbol{x}_{d1})\boldsymbol{x}_{c1} + [1 - a_1(\boldsymbol{x}_1, \boldsymbol{x}_{d1})]a_2(\boldsymbol{x}_2, \boldsymbol{x}_{d2})\boldsymbol{x}_{c2} \\
& + [1 - a_1(\boldsymbol{x}_1, \boldsymbol{x}_{d1})][1 - a_2(\boldsymbol{x}_2, \boldsymbol{x}_{d2})]a_3(\boldsymbol{x}_3, \boldsymbol{x}_{d3})\boldsymbol{x}_{c3} \\
& + [1 - a_1(\boldsymbol{x}_1, \boldsymbol{x}_{d1})][1 - a_2(\boldsymbol{x}_2, \boldsymbol{x}_{d2})][1 - a_3(\boldsymbol{x}_3, \boldsymbol{x}_{d3})] \\
& \times a_4(\boldsymbol{x}_4, \boldsymbol{x}_{d4})\boldsymbol{x}_{c4} \\
& + [1 - a_1(\boldsymbol{x}_1, \boldsymbol{x}_{d1})][1 - a_2(\boldsymbol{x}_2, \boldsymbol{x}_{d2})][1 - a_3(\boldsymbol{x}_3, \boldsymbol{x}_{d3})] \\
& \times [1 - a_4(\boldsymbol{x}_4, \boldsymbol{x}_{d4})]\boldsymbol{x}_r,
\end{aligned} \tag{8}$$

where $\boldsymbol{x}_r$ denotes a static reference position, which is also a "home" position where the gripper returns at the end of manipulation. From (8), $\boldsymbol{x}_o = \boldsymbol{x}_{c1}$ when $a_1(\boldsymbol{x}_1, \boldsymbol{x}_{d1}) = 1$, and $\boldsymbol{x}_o = \boldsymbol{x}_{c2}$ when $a_1(\boldsymbol{x}_1, \boldsymbol{x}_{d1}) = 0$ and $a_2(\boldsymbol{x}_2, \boldsymbol{x}_{d2}) = 1$, and so on. That is, $\boldsymbol{x}_o = \boldsymbol{x}_{ci}$ only when the weighting function for the ith wire becomes 1, and the weighting functions for the previous $i-1$ wires are equal to zero. Therefore, the alignment of the Red wire is of the highest priority, and that of the $Black$ wire is of the lowest priority. When all $a_i(\boldsymbol{x}_i, \boldsymbol{x}_{di})$ are equal to 0, $\boldsymbol{x}_o = \boldsymbol{x}_r$, such that the gripper returns to the "home" position and waits for the manipulation of next USB wires. The variations of $\boldsymbol{x}_o$ are summarized in Tab. I. Note that the composite vector can be easily extended to applications where more wires need to be manipulated (e.g. LAN cables), by following a similar structure in (8).

TABLE I
Variation of Composite Vector

$a_1(\cdot)$[1]	$a_2(\cdot)$	$a_3(\cdot)$	$a_4(\cdot)$	$\boldsymbol{x}_o$	Alignment
1	N.A.	N.A.	N.A.	$\boldsymbol{x}_{c1}$	Red
0	1	N.A.	N.A.	$\boldsymbol{x}_{c2}$	$White$
0	0	1	N.A.	$\boldsymbol{x}_{c3}$	$Green$
0	0	0	1	$\boldsymbol{x}_{c4}$	$Black$
0	0	0	0	$\boldsymbol{x}_r$	return to "home"

[1] where $a_i(\cdot) \triangleq a_i(\boldsymbol{x}_i, \boldsymbol{x}_{di})$

The use of the overall composite vector $\boldsymbol{x}_o$ ensures that each wire is stably fixed at the designated groove, since the robot keeps monitoring the location of the wire with respect to the groove throughout the manipulation. Whenever a wire with higher priority escapes, the current alignment is suspended and the gripper moves to re-grasp and re-manipulate that wire.

Therefore, the control objective can be specified as: $\boldsymbol{x} \rightarrow \boldsymbol{x}_o$. In particular, when $\boldsymbol{x}_o = \boldsymbol{x}_{ci}$ and $\boldsymbol{x}_{ci} = \boldsymbol{x}_i$, the control objective is $\boldsymbol{x} \rightarrow \boldsymbol{x}_i$, i.e. the gripper moves to grasp the ith wire. When $\boldsymbol{x}_o = \boldsymbol{x}_{ci}$ and $\boldsymbol{x}_{ci} = \boldsymbol{x}_{di}$, the objective becomes $\boldsymbol{x} \rightarrow \boldsymbol{x}_{di}$, and hence the grasped ith wire is manipulated to the desired position. The time derivative $\dot{\boldsymbol{x}}_o$ can be obtained by differentiating (8) with respect to time. Note that $\dot{a}(\boldsymbol{x}_i, \boldsymbol{x}_{di}) = 0$ when $a(\boldsymbol{x}_i, \boldsymbol{x}_{di})$ is equal to 0 or 1. When $0 < a(\boldsymbol{x}_i, \boldsymbol{x}_{di}) < 1$, the ith wire has already been fixed at the groove such that $\dot{\boldsymbol{x}}_i \approx 0$, and hence $\dot{a}(\boldsymbol{x}_i, \boldsymbol{x}_{di}) = \dot{\boldsymbol{x}}_i^T [\frac{\partial a(\boldsymbol{x}_i, \boldsymbol{x}_{di})}{\partial (\boldsymbol{x}_i - \boldsymbol{x}_{di})}]^T$ is bounded. Since both $\dot{a}(\boldsymbol{x}_i, \boldsymbol{x}_{di})$ and $\dot{\boldsymbol{x}}_{ci}$ are bounded, $\dot{\boldsymbol{x}}_o$ is bounded.

C. Vision-Based Control

To guarantee the convergence of $\boldsymbol{x} \rightarrow \boldsymbol{x}_o$, a vision-based controller is proposed in this section. First, a sliding vector is proposed as:

$$\begin{aligned} \boldsymbol{s} &= \dot{\boldsymbol{q}} - \dot{\boldsymbol{q}}_r \\ &= \dot{\boldsymbol{q}} - \boldsymbol{J}^+(\boldsymbol{q})\dot{\boldsymbol{x}}_o + \alpha \boldsymbol{J}^+(\boldsymbol{q})\Delta\boldsymbol{x}, \end{aligned} \tag{9}$$

where $\dot{\boldsymbol{q}}_r = \boldsymbol{J}^+(\boldsymbol{q})\dot{\boldsymbol{x}}_o - \alpha \boldsymbol{J}^+(\boldsymbol{q})\Delta\boldsymbol{x}$ is a reference vector, α is a positive constant, $\boldsymbol{J}^+(\boldsymbol{q})$ is the pseudo-inverse of $\boldsymbol{J}(\boldsymbol{q})$, and $\Delta\boldsymbol{x} = \boldsymbol{x} - \boldsymbol{x}_o$.

The control input is now proposed as:

$$\begin{aligned} \boldsymbol{\tau} = &-\boldsymbol{K}_s \boldsymbol{s} - \boldsymbol{J}^T(\boldsymbol{q})\boldsymbol{K}_p \Delta\boldsymbol{x} \\ &- k_g \boldsymbol{sgn}(\boldsymbol{s}) + \boldsymbol{M}(\boldsymbol{q})\ddot{\boldsymbol{q}}_r + \boldsymbol{C}(\dot{\boldsymbol{q}}, \boldsymbol{q})\dot{\boldsymbol{q}}_r + \boldsymbol{g}(\boldsymbol{q}), \end{aligned} \tag{10}$$

where $\boldsymbol{K}_s \in \Re^{n \times n}$ and $\boldsymbol{K}_p \in \Re^{2 \times 2}$ are diagonal and positive-definite matrices, k_g is a positive constant, and $\boldsymbol{sgn}(\cdot)$ is a sign function [19]. In (10), the first two terms include the position control and the velocity control, the third term is to deal with the interaction between the gripper and the wires, and the last three terms are the dynamic compensation.

Using the new state-dependent vector (8), the proposed controller (10) enables the robot to autonomously adjust the control object with visual feedback and thus react intelligently in the presence of deformation. Note that the acceleration information is required in $\ddot{\boldsymbol{x}}_o$, which are, hence, required in the control input (10). Observer can be constructed to eliminate the requirement of acceleration information by following the development in [20], [21].

Using the sliding vector (9) and substituting the control input (10) into the dynamic model (2), the closed-loop equation is obtained as:

$$\begin{aligned} &\boldsymbol{M}(\boldsymbol{q})\dot{\boldsymbol{s}} + (\boldsymbol{C}(\dot{\boldsymbol{q}}, \boldsymbol{q}) + \boldsymbol{K}_s)\boldsymbol{s} \\ &+ k_g \boldsymbol{sgn}(\boldsymbol{s}) + \boldsymbol{J}^T(\boldsymbol{q})\boldsymbol{K}_p \Delta\boldsymbol{x} = \boldsymbol{\tau}_e. \end{aligned} \tag{11}$$

We are now in the position to state the following theorem.

Theorem: *When the proposed controller (10) is applied to the robotic manipulation system, the closed-loop system gives rise to the convergence of $\boldsymbol{x} \rightarrow \boldsymbol{x}_o$ as $t \rightarrow \infty$, if the parameter k_g is chosen such that $k_g \geq b_e$, where b_e denotes the upper bound of $\boldsymbol{\tau}_e$.*

Proof: First, a Lyapunov-like candidate is proposed as:

$$V = \tfrac{1}{2}\boldsymbol{s}^T \boldsymbol{M}(\boldsymbol{q})\boldsymbol{s} + \tfrac{1}{2}\Delta\boldsymbol{x}^T \boldsymbol{K}_p \Delta\boldsymbol{x}. \tag{12}$$

Differentiating (12) with respect to time yields:

$$\dot{V} = \boldsymbol{s}^T \boldsymbol{M}(\boldsymbol{q})\dot{\boldsymbol{s}} + \tfrac{1}{2}\boldsymbol{s}^T \dot{\boldsymbol{M}}(\boldsymbol{q})\boldsymbol{s} + \Delta\dot{\boldsymbol{x}}^T \boldsymbol{K}_p \Delta\boldsymbol{x}. \tag{13}$$

Substituting (9) and (11) into (13) and using Property iii), we have:

$$\begin{aligned} \dot{V} &= \tfrac{1}{2}\boldsymbol{s}^T \dot{\boldsymbol{M}}(\boldsymbol{q})\boldsymbol{s} - \boldsymbol{s}^T [(\boldsymbol{C}(\dot{\boldsymbol{q}}, \boldsymbol{q}) + \boldsymbol{K}_s)\boldsymbol{s} \\ &+ k_g \boldsymbol{sgn}(\boldsymbol{s}) - \boldsymbol{\tau}_e + \boldsymbol{J}^T(\boldsymbol{q})\boldsymbol{K}_p \Delta\boldsymbol{x}] + \Delta\dot{\boldsymbol{x}}^T \boldsymbol{K}_p \Delta\boldsymbol{x} \\ &= -\boldsymbol{s}^T \boldsymbol{K}_s \boldsymbol{s} - \alpha \Delta\boldsymbol{x}^T \boldsymbol{K}_p \Delta\boldsymbol{x} - \boldsymbol{s}^T (k_g \boldsymbol{sgn}(\boldsymbol{s}) - \boldsymbol{\tau}_e). \end{aligned} \tag{14}$$

Note that $-\boldsymbol{s}^T(k_g \boldsymbol{sgn}(\boldsymbol{s}) - \boldsymbol{\tau}_e) \leq -(k_g - b_e)||\boldsymbol{s}||$. If k_g is chosen such that $-\boldsymbol{s}^T(k_g \boldsymbol{sgn}(\boldsymbol{s}) - \boldsymbol{\tau}_e) \leq 0$, $\dot{V} \leq 0$ from (14). Since $V > 0$ and $\dot{V} \leq 0$, V is bounded. Since V is bounded, $\boldsymbol{s}$ and $\Delta\boldsymbol{x}$ are bounded. Then, it is seen that $\dot{\boldsymbol{q}}_r$ is bounded, since both $\Delta\boldsymbol{x}$ and $\dot{\boldsymbol{x}}_o$ is bounded. The boundedness of $\boldsymbol{s}$ and $\dot{\boldsymbol{q}}_r$ ensures the boundedness of $\dot{\boldsymbol{q}}$ from (9). Then, the boundedness of $\dot{\boldsymbol{q}}$ ensures the boundedness of $\dot{\boldsymbol{x}}$, since $\dot{\boldsymbol{x}} = \boldsymbol{J}(\boldsymbol{q})\dot{\boldsymbol{q}}$, and $\boldsymbol{J}(\boldsymbol{q})$ is the trigonometric function of $\boldsymbol{q}$. Since both $\dot{\boldsymbol{x}}$ and $\dot{\boldsymbol{x}}_o$ are bounded, $\Delta\dot{\boldsymbol{x}} = \dot{\boldsymbol{x}} - \dot{\boldsymbol{x}}_o$ is bounded, that is, $\Delta\boldsymbol{x}$ is uniformly continuous. From (14), it can be derived that $\Delta\boldsymbol{x} \in L_2(0, +\infty)$. Therefore, it follows [4], [18], [22] that: $\Delta\boldsymbol{x} \rightarrow \boldsymbol{0}$, i.e. $\boldsymbol{x} \rightarrow \boldsymbol{x}_o$ as $t \rightarrow \infty$. Therefore, the manipulation task is realized. ■

IV. Experiment

An experimental setup of vision-based robotic manipulation system has been established in The Chinese University of Hong Kong as shown in Fig. 3, which mainly consists of an automatic soldering machine, a robot manipulator, a camera (Basler acA1300-60gc), a robotic gripper, a motion control module (PCI-1757UP, ADVANTECH), and a computer (operation system: Windows 10). The manipulator grasps then fixes the USB wires at the grooves on the conveyer belt by following the USB color code, and the soldering machine runs to solder the wires together with the heads. The robotic gripper is driven by the mechanism of wire stripping, and the clamping force is 3.7 N and its stroke is 4 mm. The open and closing of the gripper are controlled with a solenoid valve. The resolution of the camera is 1280×1024 pixel and the frame rate is 60 fps. In the experiments, the position of groove may be occluded by the gripper, and hence an offsetted desired position is employed in the experiments.

In the first experiment, all wires were not fixed at the grooves initially, and the robotic gripper was controlled to grasp then manipulate the wires, and carry out the alignment according to the color code sequentially. The

desired positions were specified as: $\boldsymbol{x}_{d1}=[531,535]^T$pixel, $\boldsymbol{x}_{d2}=[538,610]^T$pixel, $\boldsymbol{x}_{d3}=[530,665]^T$pixel, and $\boldsymbol{x}_{d4}=[531,719]^T$pixel respectively. The parameters of the regions $f_i(\boldsymbol{x},\boldsymbol{x}_i)\leq 0$ and $h_i(\boldsymbol{x}_i,\boldsymbol{x}_{di})\leq 0$ were set as $\delta_I=15$pixel and $\delta_{II}=30$pixel respectively, and the parameters in the weighting functions $w_i(\boldsymbol{x},\boldsymbol{x}_i)$ and $a_i(\boldsymbol{x}_i,\boldsymbol{x}_{di})$ were set as: $\kappa_I=\kappa_{II}=0.7$. The control parameters in (10) were set as: $\alpha=1$, $\boldsymbol{K}_s=0.1\boldsymbol{I}_3$, and $\boldsymbol{K}_p=0.5\boldsymbol{I}_2$, where $\boldsymbol{I}_3\in\Re^{3\times 3}$ and $\boldsymbol{I}_2\in\Re^{2\times 2}$ denote identity matrices. The position errors for each wire are given in Fig. 4, which shows that $Red, White, Green, Black$ wires were grasped at $t\approx 6, 16, 28, 39$ s respectively then manipulated to the desired positions. The duration of *Grasping* and *Manipulation* was around 10 s. The snapshots are shown in Fig. 5.

In the second experiment, the $Green$ wire was manually pulled away after it was grasped, to simulate the scenario that the wire falls off during the operation of *Grasping*. The parameters remained the same, and the position errors are shown in Fig. 6. When the $Green$ wire escaped from the gripper at $t\approx 25$ s, the gripper was able to re-grasp the $Green$ wire then manipulate it to the designated groove. The snapshots are shown in Fig. 7.

In the third experiment, the Red wire was manually pulled away after it was manipulated at the desired position, to simulate the scenario that the wire escapes from the groove during the operation of *Alignment*. Due to page limits, the results are not show in this paper but included in the video submission. In the video, the gripper was supposed to grasp then manipulate the $Black$ wire after the $Green$ wire settled. However, since the Red wire was pulled out of the groove, the gripper turned to re-grasping and re-manipulating the Red wire, as the priority of the Red wire is higher than that of the $Black$ wire. Experimental results show the successful implementation of the two-level operation. That is, the sequential operation at *Level-I* guarantees that each wire was grasped then fixed at the corresponding groove, and the sequential operation at *Level-II* ensures that the wires are properly aligned according to the USB color code.

V. Conclusion

In this paper, a new vision-based controller has been developed for robotic grasping and manipulation of USB wires. By specifying the control objective in a two-level structure, the proposed controller allows the robot to automatically grasp and manipulate the USB wires, and properly align the wires by following the color code. Such formulation guarantees the feasibility and the autonomous capability of the manipulation of USB wires. The stability of the closed-loop system has been rigorously proved using Lyapunov methods, and experimental results in different scenarios have been presented to demonstrate the performance of the proposed controller.

References

[1] www.cowen.com
[2] www.wire-processor.com
[3] www.youtube.com/watch?v=QblEd3pbZbI
[4] J. J. E. Slotine, and W. Li, *Applied Nonlinear Control*. Englewood Cliffs, New Jersy: Prentice Hall, 1991.
[5] C. C. Cheah and X. Li, *Task-Space Sensory Feedback Control of Robot Manipulators*, Springer, 2015.
[6] S. Tokumoto and S. Hirai, "Deformation control of rheological food dough using a forming process model," *IEEE International Conference on Robotics and Automation*, pp. 1457-1464, 2002.
[7] M. Higashimori, K. Yoshimoto, and M. Kaneko, "Active shaping of an unknown rheological object based on deformation decomposition into elasticity and plasticity," *IEEE International Conference on Robotics and Automation*, pp. 5120-5126, 2010.
[8] J. Das and N. Sarkar, "Autonomous shape control of a deformable object by multiple manipulators," *Journal of Intelligent and Robotic Systems*, vol. 62, pp. 3-27, 2011.
[9] D. Berenson, "Manipulation of deformable deformable objects without modeling and simulating deformation," *IEEE/RSJ International Conference on Intelligent Robots and Systems*, pp. 1-8, 2013.
[10] D. Navarro-Alarcon, Y.-H. Liu, J. G. Romero, and P. Li, "Model free visually servoed deformation control of elastic objects by robot manipulators," *IEEE Trans. Robot.*, 26(6):1457-1468, 2013.
[11] D. Navarro-Alarcon, Y.-H. Liu, J. Romero, and P. Li, "On the visual deformation servoing of compliant objects: Uncalibrated control methods and experiments," *Int. J. Robot. Res.*, vol. 33, no. 11, pp. 1462-1480, 2014.
[12] D. Navarro-Alarcon, H. Yip, Z. Wang, Y.-H. Liu, F. Zhong, T. Zhang, and P. Li, "Automatic 3D manipulation of soft objects by robotic arms with adaptive deformation model," *IEEE Trans. Robot.*, vol. 32, no. 2, pp. 429-441, 2016.
[13] D. Sun and Y. H. Liu, "Modeling and impedance control of a two-manipulator system handling a flexible beam," *ASME J. Dyn. Syst. Meas. Control*, vol. 119, no. 4, pp. 736-742, 1997.
[14] D. Sun, J. K. Mills, and Y. H. Liu, "Position control of robot manipulators manipulating a flexible payload," *Int. J. Robot. Res.*, vol. 18, no. 3, pp. 319-332, 1999.
[15] S. Hutchinson, G. Hager, and P. Corke, "A tutorial on visual servo control," *IEEE Trans. Robotics Automat.*, 12(5):651-670, 1996.

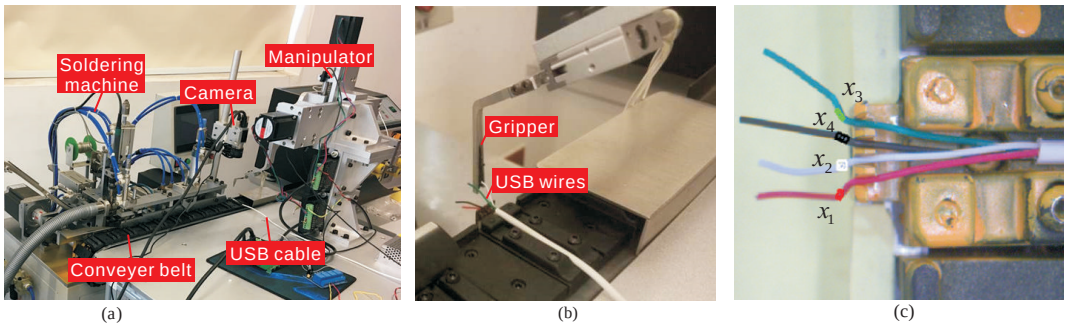

(a) (b) (c)

Fig. 3. An experimental setup of vision-based robotic manipulation system (a) The setup consists of an automatic soldering machine, a robot manipulator, a camera, a robotic gripper, a control module, and a computer; (b) The robotic gripper is controlled to manipulate the USB wires; (c) The camera is installed to detect the positions of wires.

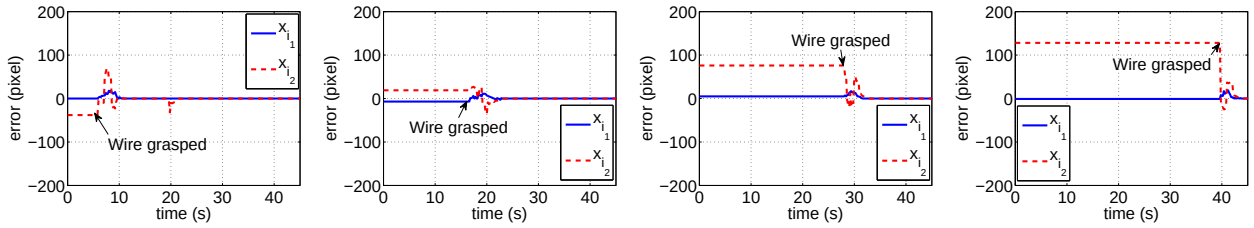

Fig. 4. Experiment 1: All wires were grasped and manipulated at the grooves by following the USB color code. (a) position errors for Red wire $\boldsymbol{x}_1-\boldsymbol{x}_{d1}$; (b) position errors for $White$ wire $\boldsymbol{x}_2-\boldsymbol{x}_{d2}$; (c) position errors for $Green$ wire $\boldsymbol{x}_3-\boldsymbol{x}_{d3}$; (d) position errors for $Black$ wire $\boldsymbol{x}_4-\boldsymbol{x}_{d4}$.

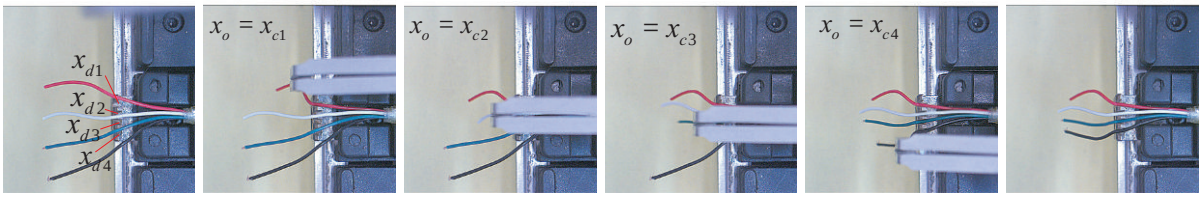

Fig. 5. Snapshots of experiment 1: (a) $t=0$ s: initial configuration; (b) $t=6$ s: grasping and manipulation of Red wire; (c) $t=16$ s: grasping and manipulation of $White$ wire; (d) $t=28$ s: grasping and manipulation of $Green$ wire; (e) $t=39$ s: grasping and manipulation of $Black$ wire; (f) $t=45$ s: final configuration.

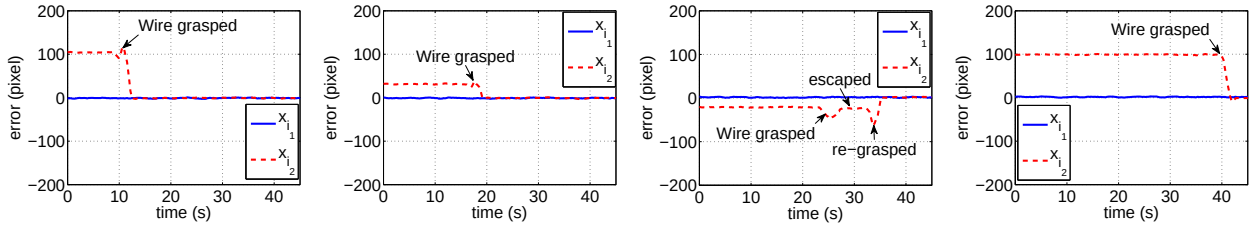

Fig. 6. Experiment 2: The $Green$ wire was manually pulled away, and the gripper re-grasped then manipulated it. (a) position errors for Red wire $\boldsymbol{x}_1-\boldsymbol{x}_{d1}$; (b) position errors for $White$ wire $\boldsymbol{x}_2-\boldsymbol{x}_{d2}$; (c) position errors for $Green$ wire $\boldsymbol{x}_3-\boldsymbol{x}_{d3}$; (d) position errors for $Black$ wire $\boldsymbol{x}_4-\boldsymbol{x}_{d4}$.

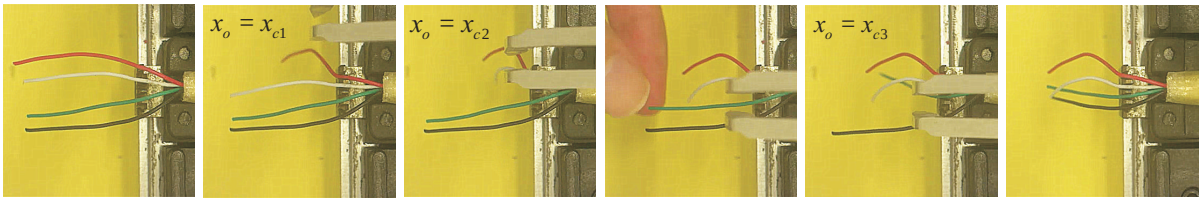

Fig. 7. Snapshots of experiment 2: (a) $t=0$ s: initial configuration; (b) $t=10$ s: grasping and manipulation of Red wire; (c) $t=18$ s: grasping and manipulation of $White$ wire; (d) $t=25$ s: $Green$ wire manually pulled away; (e) $t=34$ s: re-grasping and manipulation of $Green$ wire; (f) $t=45$ s: final configuration.

[16] Y. H. Liu, H. Wang, C. Wang, and K. K. Lam, "Uncalibrated visual servoing of robots using a depth-independent interaction matrix," *IEEE Trans. Robotics*, vol. 22, no. 4, pp. 804-817, 2006.

[17] X. Li and C. C. Cheah, "Adaptive regional feedback control of robot manipulator with uncertain kinematics and depth information," *American Control Conference*, pp. 5472-5477, 2012.

[18] S. Arimoto, *Control Theory of Non-Linear Mechanical Systems*. Oxford University Press, 1996.

[19] X. Li and C. C. Cheah, "Adaptive neural network control of robot based on a unified objective bound," *IEEE Transactions on Control Systems Technology*, vol. 22, no. 3, pp. 1032-1043, 2013.

[20] C. C. Cheah, X. Li, X. Yan and D. Sun, "Observer based optical manipulation of biological cells with robotic tweezers," *IEEE Transactions on Robotics*, vol. 30, no. 1, pp. 68-80, 2013.

[21] X. Li, Y. Pan, G. Chen, and H. Yu, "Adaptive human-robot interaction control for robots driven by series elastic actuators," *IEEE Transactions on Robotics*, vol. 33, no. 1, pp. 169-182, 2017.

[22] M. W. Spong, and M. Vidyasagar, *Robot Dynamics and Control*. New York: John Wiley & Sons, 1989.